Boletim da Sociedade Astronômica Brasileira, **34**, no. 1, 278-280

Star formation in H II galaxies

Vitor Gabriel Alves & Henri Michel Pierre Plana

[1] Programa de Pós-Graduação em Física, PROFÍSICA, Laboratório de Astrofísica Teórica e Observacional, Universidade Estadual de Santa Cruz, Ilhéus-BA e-mail: vgalves@uesc.br, plana@uesc.br

Abstract. Blue Compact Galaxies (BCGs) are classified as compact dwarf galaxies and show spectra dominated by intense emission lines superimposed on a weak continuum spectrum resembling that of H II regions. These objects are characterized by a strong star formation rate. They have the lowest metal content among most starburst objects, suggesting that they are the least evolved among known galaxies. These galaxies, are important objects of study to understand Star Formation (SF) processes and feedback effects, because they are low-mass objects with simple dynamics. We seek to understand how SF episodes occur in the absence of density waves, and to understand the role of ionized gas kinematics in the stability and evolution of SF regions. This understanding is accompanied by the study of ionization mechanisms using diagnostic diagrams and of the chemical composition of galaxies, using S-calibrator for example. The importance of feedback in SF processes was studied in an evolutionary setting. Two objects, Tol 1004-296 and Tol 0957-278, were observed using SOAR's SIFS - IFU with 4 fields of 15" x 8". These objects were chosen from different criteria, such as size, presence of the main emission lines, and high gas velocity dispersion. Two observations were made, a medium-resolution one for the different monochromatic maps and a high-resolution one for the velocity and velocity dispersion maps. From the maps of the main emission lines, we constructed diagnostic diagrams of the ionization mechanisms and oxygen abundance maps (using the S-calibrator). The kinematic diagnostic diagrams, constructed from the velocity and velocity dispersion maps, showed systematic motion around the SF sites in addition to a velocity gradient between these as well. The metallicity is higher around the SF sites compared to the centers.

Resumo. As Galáxias Compactas Azuis (Blue Compact Galaxies - BCG's) são classificadas como galáxias anãs compactas e apresentam espectros dominados por linhas de emissão intensas superpostas a um espectro contínuo fraco parecido com o de regiões H II. Esses objetos são caracterizados por uma forte taxa de formação estelar. Apresentam o menor teor de metal entre a maioria dos objetos de tipo Starburst (com forte surto de Formação Estelar), sugerindo que são as menos evoluídas entre as galáxias conhecidas. Essas galáxias, são importantes objetos de estudo para compreender os processos de Formação Estelar (FE) e efeitos de feedback, já que são objetos de baixa massa e com uma dinâmica simples. Procura-se entender como os episódios de FE ocorrem na ausência de ondas de densidade e, entender o papel da cinemática do gás ionizado na estabilidade e na evolução das regiões de FE. Essa compreensão é acompanhada pelo estudo dos mecanismos de ionização usando diagramas de diagnósticos e da composição química das galáxias, usando calibrador S por exemplo. A importância do feedback nos processos de FE foi estudada num cenário evolutivo. Dois objetos, Tol 1004-296 e Tol 0957-278, foram observados usando o SIFS - IFU do SOAR com 4 campos de 15"x8". Os objetos foram escolhidos a partir de diferentes critérios, como tamanho, presença das principais linhas de emissão e dispersão de velocidades do gás. Foram feitas duas observações, uma de resolução média, para os diferentes mapas monocromáticos e uma de alta resolução para os mapas de velocidades e de dispersão de velocidade. A partir dos mapas das principais linhas de emissão, construímos diagramas de diagnósticos dos mecanismos de ionização e mapas de abundância do oxigênio (usando o calibrador S). Os diagramas de diagnósticos cinemáticos, construídos a partir dos mapas de velocidades e de dispersão, mostraram movimentos sistemáticos ao redor dos sítios de FE além de um gradiente de velocidade entre esses também. A metalicidade é maior ao redor dos sítios de FE comparado com os centros.

Keywords. Galaxies: Star Formation – H II Galaxies – Galaxies: Kinematic and Dynamics

1. Introduction

In general, the H II galaxies (or Blue Compact Galaxies - BCG's) are classified as compact dwarf galaxies that present spectra dominated by intense emission lines, due to photoionization by the presence of a large amount of O or/and B stars (Koulouridis 2013). These intense emission lines, are overlapped on a faint continuous spectrum, similar to that of giant H II regions, which probably led them to be named in such a way (Terlevich 1991; Thuan 2008).

The main characteristic of these galaxies is their high Star Formation rate (SFR), framing them as StarBurst galaxies. In addition, they are abundant in gas with a low metallicity (Thuan 1981; Kunth 1988) having the lowest metal content among most Starburst-type objects, suggesting that they are the least evolved among known galaxies (Koulouridis 2013). They are important objects for investigating SF mechanisms, due to simple morphology and dynamics, compared to late-type objects (Hunter 2004).

By way of observations and obtaining spectral, radial velocity and velocity dispersion maps of the emission lines of two H II galaxies, Tol 1004-296 and Tol 0957-278, this work seeks to understand how the SF episodes occurred and which ionization mechanisms are involved and, in parallel, we seek to understand the effects of the ionized gas kinematics on the galaxy stability and on the evolution of the SF regions. We pretend to compare the results obtained between the two galaxies in order to highlight the differences between them and to complement the existing literature on the classification of these objects.

2. Observational Data

We use an instrument capable of obtaining 2D maps of the spectral emission lines of galaxies, the Southern Astrophysical Research Telescope (SOAR) in Chile, with an aperture of 4.2m and equipped with the SIFS-IFU[1]. In addition to emission lines,

[1] SOAR Integral Field Spectrograph

the SIFS is capable of obtaining radial velocity and dispersion velocity maps, making possible to study the gas kinematics. The SOAR observation field corresponds to 15"x8", requiring the observation of the galaxy in four fields and consequently making a mosaic with the data cubes of the observation regions.

3. Emission Lines

For the observations of the two galaxies, we used the $700M$ greating with spectral resolution of $R = 4200@5500$ Å, with which we obtained three-dimensional data cubes containing the spectra the [OIII]λ4959 Å, λ5007 Å, $H\alpha$ λ6563 Å, $H\beta$ λ4861 Å, [NII]λ6549 Å, λ6584 Å, [SII]λ6713 Å, [SII]λ6731 Å, used to estimate the values of electron density n_e, electronic temperature T_e, the oxygen abundance, the reddening due to interstellar medium (ISM) dust, and to obtain the ionization diagrams.

3.1. Eletronic Density and Temperature

The electronic density is obtained from the rate [SII]λ6713/λ6731 and the electronic temperature, from the [OIII] lines. The map of the [SII]λ6717, λ6731 shows values typically above 1, indicating a low density regime Osterbrock (2006). We then assume a constant value for $n_e = 100cm^{-3}$. It was not possible to obtain $T_{e[OIII]}$ because to the absence of the line from [OIII]λ4363. For now, we use the canonical value of 10^4K.

3.2. Reddening

To estimate the reddening due to dust, we use the $H\alpha/H\beta$ rate maps. With the density and electronic temperature conditions cited earlier, the Balmer decrement is constant (Osterbrock 2006). Using this map together with the reddening curve, we were able to correct the dust effect for the main emission lines (Calzetti 2000).

3.3. Metallicity

To measure the oxygen abundance and consequently the metallicity of galaxies, we use the method proposed by Pilyugin (2012, 2016), where we use simple expressions related to oxygen abundance ratios in regions H II with intensities of the strong lines S_2, R_3, e N_2 (S calibration): $S_2 = I_{SII}(\lambda6717 + \lambda6732)/H\beta$; $R_3 = I_{OIII}(\lambda4959 + \lambda5007)/H\beta$; $N_2 = I_{NII}(\lambda6548 + \lambda6583)/H\beta$. However, this method was only applicable for Tol 1004-296. In the case of Tol 0957-278 we used the ratio $N2 = log([NII]\lambda6584/H\alpha)$ because of the absence of the line of [NII]λ6548 (Denicolo 2002).

3.4. Ionization Diagrams

To determine the sources of excitation of the atoms in galaxies, the ratios of the strong optical emission lines are used [OIII] $\lambda5007/H\beta$ vs [NII]6584/$H\alpha$, [OIII]5007/$H\beta$ vs [SII]λ6713, 6731. Those diagnostic diagrams, called BPT diagrams, were proposed by Baldwin (1981) to distinguish between photoionized regions by H II, LINERS and objects ionized by a denser radiation field (AGN's, for example) (Kewley 2019).

4. Kinematics

For each of the lines, we extracted a sub-cube of a few dozen spectral pixels (between 30 and 40 pixels depending on the lines)

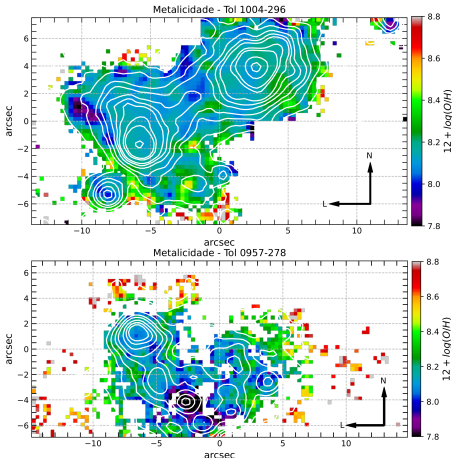

Figure 1: a) Metallicity map for the galaxy Tol 1004-296 and; (b) Tol 0957-278. The contours represent the iso-intensities of the monochromatic emission map of the Hα λ6563 Å across the observed field.

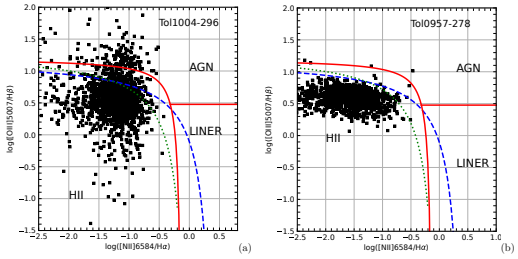

Figure 2: Ionization diagrams for (a) Tol 1004-296 and (b) Tol 0957-278. The different lines correspond in separating the three regimes: The dotted line in blue from Kewley (2001); the solid red line from Veilleux (1987); and green from Kauffmann (2003)

.

and, by isolating the emission above a certain level of the stellar continuum with a linear regression on a spectral interval for each pixel, we obtained a monochromatic image of each line. We used the most intense Hα line to obtain the radial velocity (V_r) and velocity dispersion (σ) maps. The radial velocity was determined from the barycenter of the line profile and the dispersion, estimated from the width at half height (FWHM) (Amram 1991). Corrections from Doppler and instrumental broadening, were applied to the velocity dispersion maps.

5. Results and Discussions

Figures 1, shows the metallicity maps of the two galaxies. Metallicty in two galaxies is low, with values in Tol 1004-296 ranging from $7.8 < 12 + log(O/H) < 8.6$ and in Tol 0957-278, ranging $7.8 < 12 + log(O/H) < 8.5$. However, around the SF sites, the metallicity is higher than compared to the centers, indicating higher abundance in the environment around the SF regions.

Figure 2, shows the BPT diagrams of the [OIII]5007/$H\beta$ Å vs [NII]6584/$H\alpha$ Å rates. It is noted that the responsible ionization mechanism in both galaxies is photoionization (as in a H II region). But two observations can be made: 1] diagram 2a shows that the AGN mechanism is also responsible for ionization in Tol 1004-296, while in 2b this separation is not apparent; 2] the distribution of the points in the two diagrams is radically different.

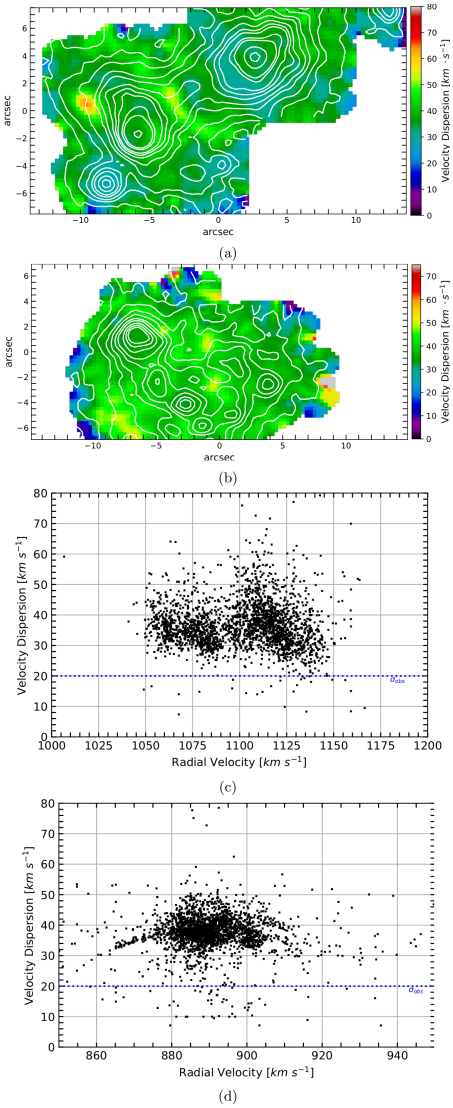

FIGURE 3: Maps of dispersion velocity Tol 1004-296 (a) and Tol 0957-278 (b); and kinematic diagnostic diagrams $\sigma - V_r$ of (c) Tol 1004-296 and (d) Tol 0957-278. The contours represent the emission iso-photes of the Hα line and the dashed line in blue, represents the observed broadening (σ_{obs}).

In 2b, the ratio [OIII]5007/$H\beta$ is much more concentrated compared to 2a.

The velocity dispersion maps (σ) and kinematic diagnostic diagrams ($\sigma - V_r$) (figure 3), show that for both cases, the velocity dispersion is greatest outside the emission centers, ranging approximately between $30km \cdot s^{-1} < \sigma < 60km \cdot s^{-1}$ in both cases. However, in Tol 0957-278, there are a greater number of regions with velocity dispersion between approximately $30km \cdot s^{-1} < \sigma < 50km \cdot s^{-1}$ at different points in the galaxy, concentrating in the interval $875km \cdot s^{-1} < V_r < 900km \cdot s^{-1}$ and spreading around it, indicating a less systemic motion of the gas in the galaxy (Bordalo 2009). In Tol 1004-296, two regions with distinct values of V_r appear in the $\sigma - V_r$ diagram, however, the points are more clustered in the intervals of $1050km \cdot s^{-1} < V_r < 1080km \cdot s^{-1}$ and $1100km \cdot s^{-1} < V_r < 1130km \cdot s^{-1}$, showing that there are regions with a velocity gradient in the galaxy. The dispersion map of Tol 1004-296, still shows a "barred" region with high velocity dispersion between the emission peaks. More detailed investigations of the dynamics around this region, will be carried out later using the 1500M network of SIFS-IFU, giving us higher spectral resolution (9500@5500 Å) for the study of the kinematics of the object in question.

6. Conclusion and Perspectives

From the results found, we conclude that the metallicity is indeed higher around the regions with high SF (high emission peaks). We have also shown that a part of the gas in the Tol 1004-296 galaxy is ionized by AGN's, and it is now up to us to identify the regions in the galaxy where ionization by AGN's occurs, and what is the relation of these regions with the kinematics (systemic) of the galaxy. The velocity dispersion map of Tol 1004-296, shows the existence of areas with high dispersion, which should be investigated with higher spectral resolution data.

Acknowledgements. We thanks the Universidade Estadual de Santa Cruz (UESC/BA), especially the Programa de Pós-graduação em Física (PROFÍSICA) and the Laboratório de Astrofísica Teórica e Observacional (LATO) for providing the necessary means to carry out this research. We thank FAPESB for the financial support, without which it would be unfeasible to accomplish such feats, and Prof. Dr. Arturo Samana, coordinator of the FAPESB INFRA PIE 0013/2016 project, for the support. We also thank Dr. Luciano Fraga of the Laboratório Nacional de Astrofísica (LNA), for the preparation of the data and the observations.

Referências

Amram P. Tese de Doutorado Observatoire de Marseille - 1991
Baldwin, J.A., Phillips, M.M., Terlevich, R. 1981, PASP, 93, 5
Bordalo, V., Plana, H., Telles, E., 2009, ApJ, 696, 1668
Calzetti, D., Armus, L., Bohlin, R.C., Kinney, A.L., Koornneef, J., 2000, ApJ, 533, 682
Denicoló, G., Terlevich, R., Terlevich, E., 2002, MNRAS, 330, 69
Hunter, D.A., Elmegreen, B.G., 2004, AJ, 128, 2170
Kauffmann, G. et al. 2003, ApJ, 346, 1055
Kewley, L.J., Dopita, M.A., Sutherland, R.S., Heisler, C.A., Trevena, J. 2001, ApJ, 556, 121
Kewley, L.J., Nicholls, D.C., Sutherland, R.S., 2019, ARA&A, 57, 511
Koulouridis, E., Plionis, M., Chávez, R., Terlevich, E., Terlevich, R., Bresolin, F., Basilakos, S., 2013, å, 554, 13
Kunth, D., Maurogosdato, S., Vigroux, L. 1988, å, 204, 10
Maza, J., Ruiz, M.T., Pena, M., Gonzalez, L.E., Wischnjewsky, M, 1991, A&A Suppl. Serie, 89, 389
Osterbrock, D.E., Ferland, G.J., 2006, Astrophysics of Gaseous Nebulae and Active Galactic Nuclei
Pilyugin, L.S., Grebel, E.K., Mattsson, L., 2012, MNRAS, 424, 2316
Pilyugin, L.S., Grebel, E.K., 2016, MNRAS, 457, 3678
Terlevich, R., Melnick, J., Masegosa, J., Moles, M., Copetti, M.V.F., 1991, A&A Suppl. Serie, 91, 285
Terlevich, E., 2011, RevMexAA, 39, 69
Thuan, T.X., Martin, G.E., 1981, ApJ, 247, 823
Thuan, T.X. 2008, Low-Metallicity Star Formation: From the First Stars to Dwarf Galaxies, Proceedings of the International Astronomical Union, IAU Symposium, Volume 255, p. 348-360
Veilleux, S., Osterbrock, D.E., 1987, ApJS, 63, 295